PROCEEDINGS OF SCIENCE

Ultra-high-energy cosmic rays from accretion shocks of galaxy clusters and filaments

Paul Simeon,[a,*] **Noémie Globus,**[b,c] **Kirk S. S. Barrow**[d] **and Roger Blandford**[e,f]

[a] *Independent,*
Los Altos, CA, USA
[b] *Department of Astronomy and Astrophysics, University of California, Santa Cruz,*
1156 High Street, Santa Cruz, CA 95064, USA
[c] *Astrophysical Big Bang Laboratory, RIKEN, Wako, Saitama, Japan*
[d] *Astronomy Department, University of Illinois at Urbana-Champaign, 1002 W Green St, Urbana, IL 61801, USA*
[e] *Kavli Institute for Particle Astrophysics and Cosmology at Stanford University,*
452 Lomita Mall, Stanford, CA 94305, USA
[f] *SLAC National Accelerator Laboratory*
2575 Sand Hill Road, Menlo Park, CA 94025, USA
E-mail: paulsimeon@gmail.com, noglobus@ucsc.edu, kbarrow@illinois.edu, rdb3@stanford.edu

The challenge of explaining the origin of ultra-high-energy cosmic rays (UHECRs) is the need for a source class that can accelerate particles up to 100 EeV and that is abundant enough to produce a near-isotropic distribution in our local universe. Accretion shocks around clusters and filaments of the cosmic web are good sources because they can naturally explain the isotropic distribution at relatively low energies, while the most massive clusters create anisotropy at the highest energies. The biggest challenge for cluster shocks has always been the need for sufficient magnetic field amplification to allow efficient diffusive shock acceleration. We argue from simulations and observations that these shocks are strong enough for cosmic rays to generate enough magnetic turbulence to reaccelerate cosmic rays to the highest energies. The shocks around galaxy filaments contribute to the isotropic flux of cosmic rays at lower energies. This model is part of a hierarchical framework of shocks that explains the evolution of the cosmic-ray composition and spectral index. Electrons accelerated at accretion shocks could account for the observed radio synchrotron background below 10 GHz.

38th International Cosmic Ray Conference (ICRC2023)
26 July - 3 August, 2023
Nagoya, Japan

ICRC2023
38th International Cosmic Ray Conference
The Astroparticle Physics Conference

*Speaker

PoS(ICRC2023)369

1. Outer accretion shocks around galaxy clusters and filaments

A full description of the acceleration, diffusion, and propagation of ultra-high-energy cosmic rays (UHECRs) in magnetic fields, inside and outside galaxies, lies beyond the reach of the current state of the field. Every source class has its strengths and weaknesses. Active galactic nuclei are favored for their immense luminosity (up to a bolometric luminosity of $10^{47}\,\mathrm{erg\,s^{-1}}$) and for the variety of ways one might conceive of tapping that power to accelerate cosmic rays up to 10^{20} eV. But the intense radiation from some of the most luminous objects in the universe poses a challenge for the fragile cosmic rays, which need to avoid photo-losses and escape from the dense environments where diffusion is slower. Furthermore, their peak power as a population was roughly at redshift $z \approx 2$, but the highest-energy cosmic rays must originate within approximately 100 Mpc, depending on the composition of the spectrum.

Diffusive shock acceleration, DSA, having been verified by observations, simulations, and in situ measurements in the Solar System, is a reliable mechanism for accelerating cosmic rays at lower energy. If one were to assume that DSA applies throughout many different shock environments from low energy to high energy, then the ultimate environments for accelerating cosmic rays to the highest energies are the largest shocks in the universe: the outer accretion shocks around large scale structure, where cold gas accretes onto galaxy clusters, filaments, and sheets. We distinguish the outer accretion shocks, which are thought to occur far outside the virial radius of clusters, from the inner accretion shocks, which occur near the virial radius and which are sometimes called virial shocks. The outer shocks are large, powerful, abundant, and enduring, exactly the qualities needed for UHECR production.

Several authors have previously examined the role of cluster and filament shocks in the acceleration of UHECRs [1–5]. The main challenge of any model of cosmic ray acceleration at accretion shocks is achieving the highest energies—up to approximately 200 EeV—with our current understanding of the strength of the magnetic field on length scales resonant with the cosmic rays, which have a gyroradius of $r_\mathrm{g} \approx 1.1\,Z\,E_\mathrm{EeV}\,B_{\mu\mathrm{G}}^{-1}$ kpc. The challenge is reduced when realizing that the spectrum drops as E^{-5} above 50 EeV. The 200 EeV cosmic rays are the top 0.1% of cosmic rays above 50 EeV, so one can choose a maximum energy of 50 EeV for a typical source environment. Iron with a rigidity of 8 EV can account for 200 EeV cosmic rays. While regions within the virial radius can have magnetic field strengths of 100–1000 nG, the plasma upstream of the accretion shocks may have field strengths around 1–100 nG, larger closer to the shock from adiabatic compression. We will show that linear theory and kinetic–fluid hybrid simulations indicate that the problem of weak magnetic fields is surmountable.

This work fits within a broader hierarchical, or multi-scale, model of cosmic ray acceleration where cosmic rays pass through a series of shocks, including stellar wind termination shocks, supernova remnant shocks, galactic wind termination shocks, and accretion shocks around large-scale structure [6]. We also consider more detailed analysis of the diffusion and escape upstream of a curved shock front.

2. Hydrodynamic simulations

We ran a hydrodynamic adaptive-mesh refinement (AMR) Enzo [7] simulation to study accretion shock dynamics around galaxy clusters. The initial conditions at $z = 100$ used cosmological parameters from Planck [8]. The simulation box had a side length of 256 co-moving Mpc h^{-1} with a 256^3 root grid of dark matter particles (mass resolution of $\sim 7 \times 10^{10}$ $M_\odot$/particle) and baryons using the code Music [9]. Given the mass resolution of the simulation, a 10^{14} $M_\odot$ dark matter gravitational potential contains ~1400 particles. We used a shock-finding algorithm [10] to detect temperature discontinuities across simulation cells and store Mach numbers as well as preshock temperatures and densities. We added a Haardt & Madau [11] background to radiatively drive a 9-species (H I, H II, He I, He II, He III, e^-, H_2, H_2^+, H^-) non-equilibrium chemistry throughout the intergalactic medium.

In this analysis, we removed shocks with Mach number less than 5 to select strong shocks that are efficient particle accelerators, and we removed shocks with preshock overdensity $\delta = \rho_b/\langle\rho_b\rangle > 10^3$ to exclude shocks deep within a cluster or a galaxy. What remains is a web of strong shocks in low-density regions, often outlining the large-scale structure of clusters, sheets, and filaments. The radius of the spherical shocks can be as large as 3 Mpc for clusters with a virial mass $\sim 10^{15} M_\odot$. Some cylindrical filaments have a radius of 1–2 Mpc, but the shapes are irregular with widening or narrowing filaments and concave shock surfaces as the filaments merge with other structures.

A typical cluster with a virial mass of $10^{14}\,M_\odot$ has a roughly spherical shock with a radius around 2 to 3 Mpc, which is around 1.5–2 times the virial radius. The typical kinetic energy processed per second by these shocks is about $10^{44}\,\mathrm{erg\,s^{-1}}$. The volume-averaged power for these selected shocks throughout the entire simulation volume is 1.0×10^{40} erg s^{-1} Mpc^{-3} (3.4×10^{-35} W m^{-3}), which is three orders of magnitude larger than the required cosmic ray luminosity density above 1 EeV (a few times 10^{44} erg Mpc^{-3} yr^{-1} (a few times 10^{-38} W m^{-3}).

3. Maximum energy

The maximum energy $E_{\rm max}$, is limited by many factors. The upstream of the source shock front needs magnetic turbulence resonant with the gyroradius $r_{\rm g}(E_{\rm max})$ for efficient acceleration. Those wave modes need an instability at that scale that grows faster than the age of the shock front (which itself is at most a Hubble time) to allow efficient confinement. In that case, the maximum energy will be limited only by the losses in the extragalctic photon backgrounds. This observational prediction is different from the usually assumed hypothesis where there is one maximum rigidity for all species. Finally, the acceleration timescale of DSA also needs to be faster than the shock lifetime.

3.1 Sufficient magnetic fields

The primary challenge with accretion shocks accelerating cosmic rays up to the highest energies is the lack of evidence of sufficient magnetic turbulence at the right scales. In this section we contend that the cosmic ray streaming instability [e.g., 12, 13] is sufficiently fast and strong to provide the necessary turbulence to scatter the highest-energy cosmic rays.

Detection of polarization fractions $\geq 20\%$ of syncrotron emission from clusters and filaments implies ordered large-scale magnetic fields [14]. These large-scale magnetic fields are measured to be 30–60 nG, with a subdominant turbulent component [15, 16]. Smaller-scale wave modes damp more quickly, leaving the larger-scale modes more prominent. Synchrotron emission is most detectable where the electron density is higher, but we guess that these ordered magnetic fields exist in the upstream environment of large-scale accretion shocks where they are amplified by the free-streaming cosmic rays. An amplification factor of 10–20 would increase the field strength to $\sim 1\,\mu$G, which is the favored value we use in our model for efficient particle acceleration.

Kinetic–fluid hybrid simulations demonstrate that strong collisionless shocks accelerate cosmic rays that amplify the magnetic turbulence in the precursor and far-upstream regions of the shock [17–19]. Those authors show that cosmic rays amplify the background magnetic field via the cosmic ray streaming instability—both the resonant and non-resonant hybrid modes, or the left-handed and right-handed circular polarizations, respectively. The initial upstream magnetic field, B_0, increases to a value, $B_{\rm tot}$, as $\langle B_{\rm tot}/B_0\rangle^2 \approx 3\xi_{cr} M_{\rm A}$, where $M_{\rm A}$ is the Alfvénic Mach number in the shock frame and $\xi_{cr} \equiv P_{cr}(r_{\rm sh})/(\rho u_-^2)$ is the ratio of cosmic ray pressure to ram pressure at the shock, typically between 10% and 15%. The accretion shocks around the largest clusters can have Mach numbers between 100 and 200, so we could expect amplification of magnetic fields by a factor of 5–10. Amplification factors could be as large as $(c/v_{\rm A})^{1/3}$ [18], which means a factor of 20 could be possible if the upstream Alfvén speed is $\sim 40\,{\rm km\,s^{-1}}$ as it may be upstream of accretion shocks.

Crucially, cosmic rays need to scatter off hydromagnetic waves at near resonance with their gyroradii. The two polarizations of the streaming instability have markedly different growth rates at length scales smaller than the gyroradius of the lowest-momentum cosmic rays in the distribution, but their behavior at very large length scales is identical [12]. The growth rate of the streaming instability, adapted from that reference, for $p \gg p_{\rm min}$ is the following: $\Gamma_{\rm SI} \approx k(p)\sqrt{\frac{3\pi}{8}\frac{\xi v_{\rm sh}^3}{Rc}}$, where $k(p) = r_g^{-1}(p)$ is the wave number resonant with cosmic rays of momentum p, $v_{\rm sh}$ is the shock speed, $\xi = 0.1$, and $R = \ln\left(\frac{p_{\rm max}}{m_{\rm i}c}\right) \approx 20$ for EeV protons. Amplification of wave modes larger than $r_{\rm g}(E_{\rm max})$ in simulation suggest that large-wavelength instabilities, like the firehose instability, may play a minor role [18].

We next calculate the growth rate and growth timescale, $\tau_{\rm growth}(k(E))$ for modes resonant with cosmic rays with energy E:

$$\Gamma_{\rm SI}(k(E)) \approx 1.3\times10^{-16}\,E_{\rm EeV}^{-1}\,v_{1000}^{3/2}\,B_{\mu\rm G}\,{\rm s^{-1}} \quad (1)$$

$$\tau_{\rm growth}(k(E)) \approx 0.24\,E_{\rm EeV}\,v_{1000}^{-3/2}\,B_{\mu\rm G}^{-1}\,{\rm Gyr}. \quad (2)$$

Equation 2 implies that wave modes that could scatter cosmic rays with rigidity of roughly 4 EV (40 EV) in 100 nG (1 μG) fields have a growth timescale of 10 Gyr if $v_{\rm sh} = 1000\,{\rm km\,s^{-1}}$. If the growth of the long-wavelength modes does not saturate too soon, the growth rate is unlikely to be a limiting factor for $E_{\rm max}$.

3.2 Sufficient time

Our simulations show that strong accretion shocks existed at least as far back as $z = 1$, or about 8 Gyr, providing a stable environment for particle acceleration. The acceleration timescale at the maximum energy, $\tau_{\rm acc}(E_{\rm max})$, must be less than the age of the shock and the energy-loss

timescale at that energy, $\tau_{\rm loss}(E_{\rm max}) \equiv -E_{\rm max}\left(\frac{dE}{dt}(E_{\rm max})\right)^{-1}$ for each species. We assume a standard DSA timescale, $\tau_{\rm acc} \simeq 8D_{\rm u}/V_{\rm sh}^2$ [20], with Bohm diffusion in the amplified field, supported by simulations of particle acceleration [19]. Assuming our fiducial values for the relevant parameters, the characteristic acceleration timescale for UHECRs is about 1 Gyr:

$$\tau_{\rm acc} \approx 850\, Z^{-1}\left(\frac{E}{1\,{\rm EeV}}\right)\left(\frac{V_{\rm sh}}{1000\,{\rm km\,s^{-1}}}\right)^{-2}\left(\frac{B_{\rm tot}}{1\,\mu{\rm G}}\right)^{-1}\kappa_{\rm B}\,{\rm Myr}, \tag{3}$$

where $\kappa \equiv D(E)/D_{\rm B}(E) = 1$ for Bohm diffusion. This acceleration timescale leaves out the effects of the curved shock front and the adiabatic and second-order acceleration that occurs upstream. Nonetheless, it is a conservative estimate of the required timescale.

Figure 1 shows the acceleration timescale plotted against rigidity, assuming magnetic turbulence at the appropriate scales of 1 μG and different shock speeds. One can find the maximum rigidity on Fig. 1 where the acceleration time curve crosses the loss time curve. Likewise, we rearrange Eq. 3 and evaluate where $\tau_{\rm acc}(E_{\rm max}) = \tau_{\rm loss}(E_{\rm max})$ to get

$$E_{\rm max} \approx 2.4\, Z\left(\frac{\tau_{\rm acc}}{2\,{\rm Gyr}}\right)\left(\frac{V_{\rm sh}}{1000\,{\rm km\,s^{-1}}}\right)^{2}\left(\frac{B_{\rm tot}}{1\,\mu{\rm G}}\right)\kappa_{\rm B}^{-1}\,{\rm EeV}. \tag{4}$$

Large galaxy clusters in our simulation often showed a range of shock speeds, sometimes surpassing 2000 km s^{-1}, where the magnetic energy density should be similarly higher. Energy losses limit all medium and heavy nuclei to 2–4 EV, which achieves the goal of 50–100 EeV with iron.

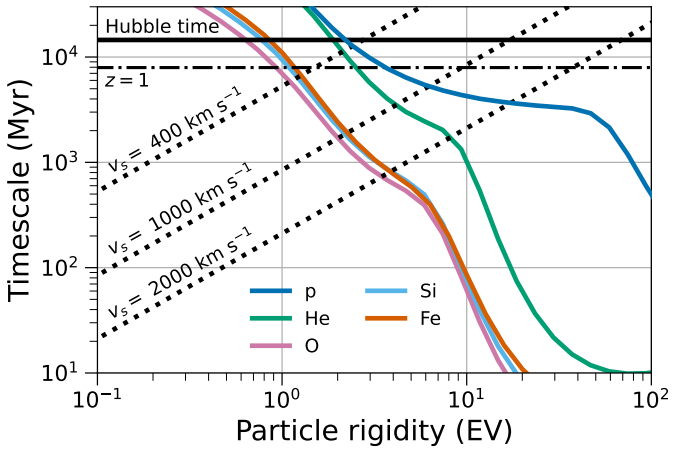

Figure 1: Acceleration timescales (dotted) for shock speeds of 400, 1000, and 2000 km s^{-1} and loss timescales (solid, colored) for protons, helium, oxygen, silicon, and iron. The upstream amplified magnetic field at the length scales resonant with the cosmic rays is assumed to be $B_{\rm tot} = 1\,\mu$G. The solid black line marking the Hubble time represents adiabatic expansion losses and the time limit for almost any source. The dash-dotted line is the elapsed cosmic time since $z = 1$.

Protons can reach a higher rigidity—perhaps 10 EV—if limited by energy losses. But protons may be advected downstream on a timescale $r_{\rm sh}/V_{\rm sh} \sim 2$ Gyr, which is shorter than the loss time at that the highest energies.

4. Observables

Downstream flux from local shocks is soft and light spectra with a relatively low rigidity cutoff. Upstream flux from cluster shocks is harder with a higher maximum rigidity. Protons (and to some extent helium nuclei) have higher rigidity cutoff than heavier nuclei, but the extra factor of Z and the lower spectral index gives the upstream flux a heavier mean composition. These two extragalactic populations are similar to the latest models from the Pierre Auger Collaboration [21].

Anisotropy in the arrival direction comes from local large-scale structures, especially from the Virgo Cluster, but we do not expect point sources or large excesses pointing at any single cluster for several reasons. First, the large extent of nearby accretion shocks smears out the flux from any source near enough to minimize deflection by intergalactic magnetic fields. Second, the previously mentioned intergalactic magnetic fields nearby large-scale structure scatter cosmic rays as they propagate through the cosmic web. Lastly, the Galactic magnetic fields deflect UHECRs before their arrival at Earth.

Accretion shocks—too faint for direct observation with existing telescopes—could be visible collectively by the radio synchrotron emission from accelerated electrons. Indeed, observations of a radio synchrotron background between 22 MHz and 10 GHz lack a consensus explanation [22].

Following the procedure in [22], the energy density in the radio background per frequency dex at ν_r is $[\nu_{\rm r} U_{\nu_{\rm r}}] = 1.17\,\frac{8\pi k_{\rm B}\nu_*^3}{c^3}\left(\frac{\nu_{\rm r}}{\nu_*}\right)^{0.4}$, where $\nu_* = 1$ GHz. When integrated up to 10 GHz, this is an energy density of $1.1\times10^{19}\,{\rm J\,m^{-3}}$. The radio synchrotron energy density relates to the emissivity j_{ν_r} of the relativistic electrons as follows:

$$[\nu_{\rm r} U_{\nu_{\rm r}}] = [\nu_{\rm r} j_{\nu_{\rm r}}]\frac{4\pi}{H_0}\int \frac{F_{\rm syn}(z)dz}{(1+z)^{(p+1)/2}E(z)}, \tag{5}$$

where $F_{\rm syn}(z)$ describes the evolution of the product $U_B \times k_e$ and $E(z) \equiv \sqrt{\Omega_M(1+z)^3+\Omega_\Lambda}$. We set $F_{\rm syn}(z) = 1$, assuming this factor is of order unity. We use the same cosmological parameters as in our simulation. We integrate up to $z = 1$, but integrating throughout all time hardly affects the answer. We solve for $[\nu_{\rm r} j_{\nu_{\rm r}}]$ and integrate over the same frequency range as above to get the power density of the relativistic electrons to be $4.2\times10^{-38}\,{\rm W\,m^{-3}}$, or 0.12% of the cosmological average power density of large-scale shocks at $z = 0$. Using the electron-to-proton energy ratio of $\eta_{\rm e} \approx 0.05$ and a cosmic-ray efficiency of $\eta_{\rm CR} \approx 0.1$, the power density put into relativistic electrons is $\mathcal{L}_{\rm e} \approx \eta_{\rm e}\eta_{\rm CR}\mathcal{L}_{\rm sh} \approx 3.5\mathcal{L}_{\rm RSB}$. While there is certainly some evolution to the power density of large-scale shocks, we expect the evolution to by relatively flat up to $z = 1$.

As with the arrival of cosmic rays, the angular anisotropy of the radio emission from accretion shocks provides another method to discriminate accretion shocks from other point-like sources. This work will be the subject of a future publication.

5. Conclusions

Despite previous concerns about accelerating cosmic rays to the highest energies, accretion shocks remain a viable candidate for a primary source of UHECRs. The cosmic web of accretion shocks is a ubiquitous and long-lasting source of extragalactic cosmic rays reaccelerated after escaping from galaxies.

We ran hydrodynamic simulations to estimate the power of these shocks and their characteristics. Shock power is not a problem *if* the cosmic rays can convert enough gas kinetic energy into magnetic turbulence. We cite previous literature finding collisionless shocks can convert upstream gas flow into cosmic ray pressure and magnetic turbulence through mutual interaction between the two nonthermal components. The growth timescale for the cosmic ray streaming instability is shorter than the required acceleration timescale, which itself is shorter than the relevant loss timescale for each species.

We show that accretion shocks around large clusters can accelerate heavy cosmic rays to 50–100 EeV, but the slower shock speeds around filaments and sheets are still excellent sources of lower-energy cosmic rays. Accretion shocks can distinguish themselves from other sources by their unique characteristics of the energy spectrum, composition, anisotropy, and electron radio synchrotron emission.

References

[1] C.A. Norman, D.B. Melrose and A. Achterberg, *The Origin of Cosmic Rays above 10 18.5 eV*, ApJ **454** (1995) 60.

[2] H. Kang, D. Ryu and T.W. Jones, *Cluster Accretion Shocks as Possible Acceleration Sites for Ultra–High-Energy Protons below the Greisen Cutoff*, ApJ **456** (1996) 422 [astro-ph/9507113].

[3] S. Inoue, G. Sigl, F. Miniati and E. Armengaud, *Ultrahigh energy cosmic rays as heavy nuclei from cluster accretion shocks*, *arXiv e-prints* (2007) astro [astro-ph/0701167].

[4] M.A. Malkov, R.Z. Sagdeev and P.H. Diamond, *UHECR acceleration in dark matter filaments of cosmological structure formation*, J. Cosmology Astropart. Phys. **2011** (2011) 024 [1101.4958].

[5] P.E. Simeon, *On the acceleration, dynamics, and propagation of cosmic rays*, Ph.D. thesis, Stanford University, 2014.

[6] R. Blandford, P. Simeon, N. Globus, P. Mukhopadhyay, E. Peretti and K.S.S. Barrow, *A hierarchical framework for explaining the cosmic ray spectrum using diffusive shock acceleration*, in *Proceedings of 38th International Cosmic Ray Conference — PoS(ICRC2023)*, vol. 444, p. 127, 2023, DOI.

[7] G.L. Bryan, M.L. Norman, B.W. O'Shea, T. Abel, J.H. Wise, M.J. Turk et al., *ENZO: An Adaptive Mesh Refinement Code for Astrophysics*, ApJS **211** (2014) 19 [1307.2265].

[8] Planck Collaboration, N. Aghanim, Y. Akrami, M. Ashdown, J. Aumont, C. Baccigalupi et al., *Planck 2018 results. VI. Cosmological parameters*, A&A **641** (2020) A6 [1807.06209].

[9] O. Hahn and T. Abel, *Multi-scale initial conditions for cosmological simulations*, MNRAS **415** (2011) 2101 [1103.6031].

[10] S.W. Skillman, B.W. O'Shea, E.J. Hallman, J.O. Burns and M.L. Norman, *Cosmological Shocks in Adaptive Mesh Refinement Simulations and the Acceleration of Cosmic Rays*, ApJ **689** (2008) 1063 [0806.1522].

[11] F. Haardt and P. Madau, *Radiative Transfer in a Clumpy Universe. IV. New Synthesis Models of the Cosmic UV/X-Ray Background*, ApJ **746** (2012) 125 [1105.2039].

[12] E. Amato and P. Blasi, *A kinetic approach to cosmic-ray-induced streaming instability at supernova shocks*, MNRAS **392** (2009) 1591 [0806.1223].

[13] A. Marcowith, A.J. van Marle and I. Plotnikov, *The cosmic ray-driven streaming instability in astrophysical and space plasmas*, *Physics of Plasmas* **28** (2021) 080601.

[14] T. Vernstrom, J. West, F. Vazza, D. Wittor, C.J. Riseley and G. Heald, *Polarized accretion shocks from the cosmic web*, *Science Advances* **9** (2023) eade7233 [2302.08072].

[15] T. Vernstrom, G. Heald, F. Vazza, T.J. Galvin, J.L. West, N. Locatelli et al., *Discovery of magnetic fields along stacked cosmic filaments as revealed by radio and X-ray emission*, MNRAS **505** (2021) 4178 [2101.09331].

[16] E. Carretti, V. Vacca, S.P. O'Sullivan, G.H. Heald, C. Horellou, H.J.A. Röttgering et al., *Magnetic field strength in cosmic web filaments*, MNRAS **512** (2022) 945 [2202.04607].

[17] D. Caprioli and A. Spitkovsky, *Simulations of Ion Acceleration at Non-relativistic Shocks. I. Acceleration Efficiency*, ApJ **783** (2014) 91 [1310.2943].

[18] D. Caprioli and A. Spitkovsky, *Simulations of Ion Acceleration at Non-relativistic Shocks. II. Magnetic Field Amplification*, ApJ **794** (2014) 46 [1401.7679].

[19] D. Caprioli and A. Spitkovsky, *Simulations of Ion Acceleration at Non-relativistic Shocks. III. Particle Diffusion*, ApJ **794** (2014) 47 [1407.2261].

[20] A.R. Bell, *Cosmic ray acceleration*, *Astroparticle Physics* **43** (2013) 56.

[21] A. Abdul Halim, P. Abreu, M. Aglietta, I. Allekotte, K. Almeida Cheminant, A. Almela et al., *Constraining the sources of ultra-high-energy cosmic rays across and above the ankle with the spectrum and composition data measured at the Pierre Auger Observatory*, J. Cosmology Astropart. Phys. **2023** (2023) 024 [2211.02857].

[22] J. Singal, Ł. Stawarz, A. Lawrence and V. Petrosian, *Sources of the radio background considered*, MNRAS **409** (2010) 1172 [0909.1997].

PoS(ICRC2023)369